Generalized Multimode Scattering Parameters and the Applications in Antenna and RF Component Designs

Siyu Li[1], Shaowei Liao[2], Wenquan Che[2], Quan Xue[2]

[1]School of Engineering and Digital Arts, University of Kent, Canterbury CT2 7NT, United Kingdom.
[2]Guangdong Provincial Key Laboratory of Millimeter-Wave and Terahertz, School of Electronic and Information Engineering, South China University of Technology, Guangzhou 510641, China.

Correspondence

Guangdong Provincial Key Laboratory of Millimeter-Wave and Terahertz, the School of Electronic and Information Engineering, South China University of Technology, Guangzhou 510641, China. (Corresponding author: Shaowei Liao, Email: liaoshaowei@scut.edu.cn).

Abstract

This paper applies the generalized multimode *S*-parameters to multiport antennas and RF components for CAD applications. Consider the special case of impedance matching which could significantly simplify the multimode representation on port and remove the requirement on calculating port impedance. *N* single-ended ports of a network are regarded as one generalized multimode port, supporting *N* orthonormal modes represented by *N* orthonormal basis vectors, respectively. By doing this, in antenna and RF component designs, one can only focus on specific modes interested, while ignore others. A multiport network's characteristics could be represented and understood in a much simpler manner because fewer but more intuitive physical quantities are considered. Therefore, this can significantly simplify the analysis, design, and optimization of multiport networks. For better illustration, several examples, including branch-line coupler, mixed-mode case, sequential rotation feeding antenna, and monopulse feed are analyzed and designed. Complicated analyses in network design using the single-ended *S*-parameters, including matching, amplitude and phase unbalance, could be converted into much simpler ones from the generalized multimode perspective.

KEYWORDS

computer-aided design (CAD), mixed-mode, multimode, scattering parameters (*S*-parameters),

1 INTRODUCTION

The mixed-mode *S*-parameters regard two single-ended ports of the same type as one mixed-mode port supporting two orthonormal modes, i.e., common and differential modes[1]. Since their introduction by Bockelman and Eisenstadt in 1995[2], a series of works have been done to complete the mixed-mode *S*-parameters theory[3,4]. The mixed-mode *S*-parameters significantly simplify various differential antennas, components, circuits, and integrated circuit (IC) designs than the traditional single-ended *S*-parameters. For example, the impedance matching evaluation of differential antennas such as dielectric antenna[5], dipole antenna[6], and array[7] could become much more straightforward and intuitive. In particular, in 2020, an antenna array decoupling method based on differential- and common-mode cancellation was proposed, giving a new perspective and path for the mixed-mode *S*-parameters applications[8]. Balanced bandpass filters[9] and balanced coupled lines[10] also apply the mixed-mode *S*-parameters to discuss differential- and common-mode responses and suppress common-mode noise. Besides, the mixed-mode *S*-parameters are also handy for various differential RF IC designs[11-13].

Inspired by the mixed-mode *S*-parameters' concept, in 2015, Meyer and Prinsloo extended the *S*-parameters to a more general situation, which they called the generalized multimode *S*-parameters[14]. In the work, the authors presented a completely general approach to the transformation of the *S*-parameters between two *N*-port networks. The equivalent port voltages and currents on one network can be made up of arbitrary combinations of, respectively, the port voltages and currents of the other network, with arbitrary real-valued port impedances on both networks. It was also shown the mixed-mode situations (the case of differential and common modes combinations)[2-4] could also be regarded as specific cases of the multimode networks. As an example of application, a quadraxial feed cross-dipole antenna matching and radiation pattern were analyzed and verified using the multimode theory. Before the publication of Ref. 14, the same authors used the concept of the multimode *S*-parameters in the design of quad-mode cross dipole antenna[15].

In Ref. 14, Meyer and Prinsloo preliminarily developed a process for evaluating the matching and radiation pattern for multiport networks using the generalized multimode *S*-parameters. However, the theory in Ref. 14 is based on circuit theory, thus, to use the generalized multimode *S*-parameters, port impedances for all ports (both single-ended and multimode ports) must be available, and should be real-valued. This seriously restricts the application of the generalized multimode *S*-parameters, in particular for waveguide and lossy transmission line as there is no well-defined impedance for waveguide, and lossy transmission line's port impedance is complex. In addition, the case of perfectly matched excitation port is always considered in modern electromagnetic (EM) CAD applications, where the port impedance is not needed to be considered. Besides, only two simple examples were given in Ref. 14, which do not fully demonstrate the generalized multimode *S*-parameters' compatibility.

The generalized multimode *S*-parameters analysis method in Ref. 14 can be further developed and applied for CAD applications. The requirement on calculating port impedance of the generalized multimode *S*-parameters can be removed and not be considered for most CAD simulation cases as the excitation ports (such as the wave port in Ansys HFSS and the waveguide port in CST Studio Suite) are naturally perfectly matched in practical designs. In fact, the concept of the generalized multimode *S*-parameters has been

applied in the analysis and design of 3- and 4-element sequential rotation feeding (SRF) antennas in Refs. 16, 17, where port impedance is not required. Reflection/transmission coefficient in terms of the orthonormal mode corresponding to the left-hand circular polarization (LHCP) radiation has been derived and evaluated, significantly simplifying the analysis and designs of two SRF antennas' radiators and feeding networks. However, in Refs. 16, 17, the analysis is restricted to 3 and 4 single-ended ports of the same type, respectively, and only one orthonormal mode (corresponding to the LHCP radiation) is considered. For general cases with multiple single-ended ports ($\geqslant 2$ ports), such as multiport radiator and feeding network, a general and practical method based on the generalized multimode *S*-parameters for multiport networks in CAD applications should be developed.

Inspired by Meyer and Prinsloo's theory[14] and similar work in Refs. 16, 17, This paper applies the generalized multimode *S*-parameters in designing and analyzing the multiport antennas and RF components for CAD applications. Consider the special case of impedance matching which could significantly simplify the multimode representation on port, and remove the requirement on calculating port impedance. N single-ended ports of a network are regarded as one generalized multimode port, supporting N orthonormal modes represented by N orthonormal basis vectors, respectively. Multiport networks that are difficult to be solved or understood in single-ended manners then could be converted into much simpler multimode reflection and transmission analysis from the multimode perspective. In this way, one can only focus on the modes interested and ignore others, which leads to fewer but more intuitive physical quantities needed to be considered. This would significantly simplify the analysis, design, and optimization of some RF/microwave multiport networks. Several design examples, including a conventional 3-dB 90° branch-line coupler, the standard mixed-mode case, an SRF LHCP antenna, and a monopulse feed are designed and analyzed using commercial EM CAD software Ansys HFSS with the proposed method.

The remainder of this paper is arranged as follows. Section 2 defines the generalized multimode port and deduce the transformation between the single-ended and generalized multimode *S*-parameters based on the premise of perfectly matched port. The analysis procedure using the generalized multimode *S*-parameters is listed at the end of the section. Section 3 presents a simple but representative example of a 3-dB 90° branch-line coupler analyzed using the generalized multimode *S*-parameters to explain the method briefly. In Section 4, the standard mixed-mode case is analyzed and verified using the proposed method, which shows good compatibility with the mixed-mode theory. Then an SRF LHCP antenna, including the radiator, corresponding feeding network, and whole combined structure, is illustrated in Section 5. In Section 6, a monopulse feed is analyzed using the similar manner with previous sections. At last, a brief discussion is shown in Section 7. The appendix briefly gives the fundamental mathematical theory used in this paper.

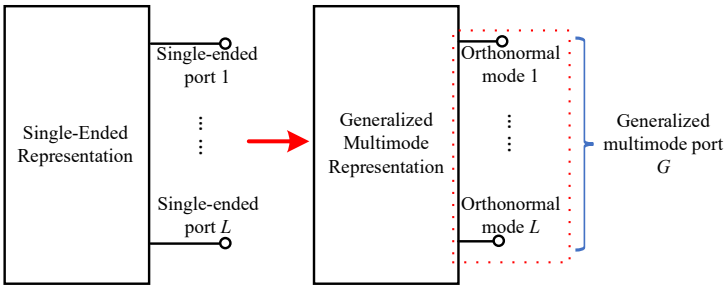

Figure 1 *L* single-ended ports of the same type (i.e., either input or output ports with equal status) are mapped into a generalized multimode port which supports *L* orthonormal modes.

2 Generalized Multimode S-Parameters

This section aims to re-derive the generalized multimode *S*-parameters based on the premise of perfectly matched port and give the general approach for design and analysis. First the generalized multimode port is defined which supports N orthonormal modes represented by N orthonormal basis vectors, respectively. Appropriate orthonormal mode definitions can significantly simplify the analysis and design of a microwave network. Once the orthonormal modes of all the generalized multimode ports are obtained, the transformation between the single-ended and generalized multimode *S*-parameters of a microwave network can be derived. The result shows a good consistency with the formula deduced in Ref. 14. At last, at the end of this section, the general procedure of using the generalized multimode *S*-parameters to design and analyze a microwave network is given.

2.1 Generalized Multimode Port, Its Orthonormal Modes and Orthonormal Basis

Here, assume all the ports of a microwave network are terminated with loads matched with the corresponding port TLs, and thus there will be no reflection between the port and port TL. Please note, based on field theory, such as CAD software for 3D EM field simulation, matched loads corresponding to the field matching rather than impedance matching are usually realized by using perfectly matched layers (PMLs) or absorbing boundary conditions (ABCs)[18].

A mixed-mode port is formed by two single-ended ports of the same type, which can support two orthonormal modes, i.e., differential and common modes[19]. The two orthonormal modes form an orthonormal basis describing the mixed-mode port. Though

two orthonormal modes are not unique, and so is the orthonormal basis, defining differential and common modes can significantly simplify the analysis and design of various differential microwave networks.

Extend the mixed-mode port concept to a more general case and defines a generalized multimode port G formed by L single-ended ports of the same type (i.e., either input or output single-ended ports with the equal status) of a network, as shown in Figure 1. Assume that all the single-ended ports only support one propagation mode (such as TEM mode for TEM TLs, TE_{10} mode for rectangular waveguide), which applies to most cases. Thus, the generalized multimode port G can support L orthonormal modes, since having L degrees of freedom (DoFs). An arbitrary unitless complex amplitude on the generalized multimode port G can be represented by the superposition of these L orthonormal modes. The corresponding modes form an orthonormal basis defining the generalized multimode port G (which is equivalent to a L-D vector space). There are infinite different orthonormal bases for the same generalized multimode port G.

Now, consider the expressions of orthonormal mode and basis. The pth orthonormal mode on the generalized multimode port G is denoted as vector $\boldsymbol{u}_{G:p}$ $(p = 1, 2, \dots, L)$, which is defined in terms of the single-ended port, given by,

$$\boldsymbol{u}_{G:p} = [x_{p1} \quad x_{p2} \quad \cdots \quad x_{pL}]^{\mathrm{T}} \tag{1}$$

where x_{pi} represents unitless complex amplitude on the ith single-ended port. Then the orthonormal basis formed by all the L orthonormal modes for the generalized multimode representation is given by

$$\boldsymbol{B}^{MM} = [\boldsymbol{u}_{G:1} \quad \boldsymbol{u}_{G:2} \quad \cdots \quad \boldsymbol{u}_{G:L}]_{L\times L}. \tag{2}$$

Please note that $\boldsymbol{B}^{MM}$ is not unique for the same microwave network, which depends on the orthonormal mode definitions. For a specific microwave network, appropriate orthonormal mode definitions can significantly simplify the analysis and design.

In particular, when $\boldsymbol{B}^{MM}$ is a unit matrix, it degenerates to the single-ended representation and thus is named as $\boldsymbol{B}^{SE}$, namely

$$\boldsymbol{B}^{SE} = \boldsymbol{I}_{L\times L}. \tag{3}$$

An arbitrary power wave amplitude on the same ports of a microwave network can be expressed as either $\boldsymbol{d}^{SE}$ or $\boldsymbol{d}^{MM}$, for the single-ended or generalized multimode representation, respectively. Both $\boldsymbol{d}^{SE}$ and $\boldsymbol{d}^{MM}$ are L-D column vectors, and each element represents the power wave amplitude on the corresponding single-ended ports and orthonormal modes, respectively. Since $\boldsymbol{B}^{MM}$ is defined in terms of the single-ended port, $\boldsymbol{d}^{SE}$ and $\boldsymbol{d}^{MM}$ can be related by,

$$\boldsymbol{d}^{SE} = \boldsymbol{B}^{MM}\boldsymbol{d}^{MM} \tag{4-1}$$

or

$$\boldsymbol{d}^{MM} = (\boldsymbol{B}^{MM})^{-1}\boldsymbol{d}^{SE}. \tag{4-2}$$

Once having (4), the transformation between the single-ended and generalized multimode S-parameters can be deduced, which will be discussed in the next part.

2.2 Transformation Between Single-Ended and Generalized Multimode S-Parameters

Let $\boldsymbol{S}^{SE}$ and $\boldsymbol{S}^{MM}$ be the single-ended and generalized multimode S-parameters for the same microwave network, respectively. $\boldsymbol{S}^{SE}$ represents the transmissions and reflections on the single-ended port(s) of the microwave network, and $\boldsymbol{S}^{MM}$ represents the transmissions and reflections of the *orthonormal modes* on the generalized multimode port. For the single-ended port representation, let $\boldsymbol{a}^{SE}$ and $\boldsymbol{b}^{SE}$ be the unitless complex amplitudes of incident and reflected waves on the single-ended ports, respectively. Similarly, for the generalized multimode port representation, let $\boldsymbol{a}^{MM}$ and $\boldsymbol{b}^{MM}$ be the unitless complex amplitudes of incident and reflected waves on the generalized multimode port, respectively. Then one can obtain the following relations from the S-parameters definition,

$$\boldsymbol{b}^{SE} = \boldsymbol{S}^{SE}\boldsymbol{a}^{SE} \tag{5-1}$$
$$\boldsymbol{b}^{MM} = \boldsymbol{S}^{MM}\boldsymbol{a}^{MM}. \tag{5-2}$$

From (4), one has

$$\boldsymbol{b}^{MM} = (\boldsymbol{B}^{MM})^{-1}\boldsymbol{b}^{SE} \tag{6-1}$$
$$\boldsymbol{a}^{MM} = (\boldsymbol{B}^{MM})^{-1}\boldsymbol{a}^{SE}. \tag{6-2}$$

Then, considering (5) and (6), the relation between the single-ended and generalized multimode S-parameters can be obtained as follow,

$$\boldsymbol{S}^{MM} = (\boldsymbol{B}^{MM})^{-1}\boldsymbol{S}^{SE}\boldsymbol{B}^{MM}. \tag{7}$$

Since $\boldsymbol{B}^{MM}$ is an orthonormal matrix, it meets following relation,

$$(\boldsymbol{B}^{MM})^{-1} = (\boldsymbol{B}^{MM})^{\dagger} \tag{8}$$

where the superscript † represents the conjugate transpose operator. Then (8) could be simplified as follow,

$$\boldsymbol{S}^{MM} = (\boldsymbol{B}^{MM})^{\dagger}\boldsymbol{S}^{SE}\boldsymbol{B}^{MM}. \tag{9}$$

The single-ended *S*-parameters $\boldsymbol{S}^{SE}$ of a microwave network is easy to obtain from EM simulation or measurement. Hence, once $\boldsymbol{S}^{SE}$ is available, the generalized multimode *S*-parameters $\boldsymbol{S}^{MM}$ can be calculated from (9). Each element's meaning of $\boldsymbol{S}^{MM}$ will be introduced in examples in the following sections.

Please note that: 1) defining appropriate orthonormal modes on the generalized multimode port to form an appropriate orthonormal basis $\boldsymbol{B}^{MM}$ can significantly simplify the analysis and design of a specific microwave network. This will be shown in the next sections. 2) Port impedance is not required when transform the single-ended S-parameters to generalized multimode ones thanks to the premise of considering the special case of perfectly matched port.

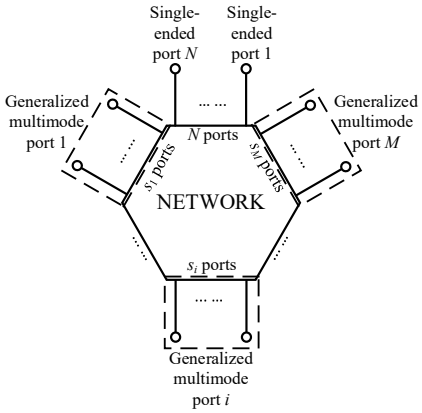

Figure 2 An arbitrary microwave network having *N* single-ended ports and *M* generalized multimode ports. The *i*th generalized multimode port is formed by s_i single-ended ports.

2.3 Microwave Network with Multiple Generalized Multimode Ports and/or Single-Ended Ports

In the previous part, the microwave network with only one generalized multimode port and without single-ended port is discussed. Nevertheless, (9) can also be extended to the microwave networks with multiple generalized multimode ports and/or single-ended ports.

Consider an arbitrary microwave network having *N* single-ended ports and *M* generalized multimode ports, as shown in Figure 2. The *i*th generalized multimode port is formed by s_i single-ended ports, and its orthonormal basis containing the s_i orthonormal modes is $\boldsymbol{B}_i$. Here, the mixed-mode port is also considered as a generalized multimode port. Then, the orthonormal basis $\boldsymbol{B}^{MM}$ for the entire microwave network is obtained as follow,

$$\boldsymbol{B}^{MM} = \begin{bmatrix} \boldsymbol{I}_{N\times N} & & & \\ & \boldsymbol{B}_1 & & \boldsymbol{0} \\ & & \ddots & \\ & & & \boldsymbol{B}_i \\ & \boldsymbol{0} & & & \ddots \\ & & & & & \boldsymbol{B}_M \end{bmatrix}_{(N+\sum_{i=1}^{M} s_i)\times(N+\sum_{i=1}^{M} s_i)}. \tag{10}$$

Once the orthonormal basis $\boldsymbol{B}^{MM}$ is obtained. One can apply (9) to acquire the generalized multimode *S*-parameters $\boldsymbol{S}^{MM}$ for the overall microwave network from the corresponding single-ended *S*-parameters $\boldsymbol{S}^{SE}$.

2.4 Analysis Procedure Using Generalized Multimode S-Parameters

According to the theory given in the previous parts, the analysis procedure for a given microwave network is as follows,

Step 1 Defining the generalized multimode port: Map the single-ended representation of the microwave network to the generalized multimode one by taking the single-ended ports of the same type as one generalized multimode port.

Step 2 Determining the orthonormal basis $\boldsymbol{B}^{MM}$: Regarding to the practical application, define orthonormal modes to form the orthonormal basis $\boldsymbol{B}_i$ for the *i*th generalized multimode port, and then the orthonormal basis $\boldsymbol{B}^{MM}$ of the overall generalized multimode network using (10). Appropriate orthonormal modes will make the analysis have clear physical meanings and insight information, thus significantly simplify the design and analysis of the network.

Step 3 Obtaining the generalized multimode *S*-parameters $\boldsymbol{S}^{MM}$: Applying (9), obtain the generalized multimode *S*-parameters $\boldsymbol{S}^{MM}$ of the microwave network from the single-ended ones $\boldsymbol{S}^{SE}$.

Step 4 Analysis using the generalized multimode *S*-parameters $\boldsymbol{S}^{MM}$: Analyze the microwave network utilizing the generalized multimode *S*-parameters $\boldsymbol{S}^{MM}$ from the perspective of generalized multimode ports rather than single-ended ports.

For better illustration and showing the advantage of the generalized multimode *S*-parameters, some examples on microwave component design based on commercial CAD software Ansys HFSS will be given in the following sections using the proposed method and method. Note that for simplification but not confusion, in the following illustration $\boldsymbol{S}^{SE}$ would represent different dimension single-ended *S*-parameters in different cases, and the variables used in each following section only apply to the section itself.

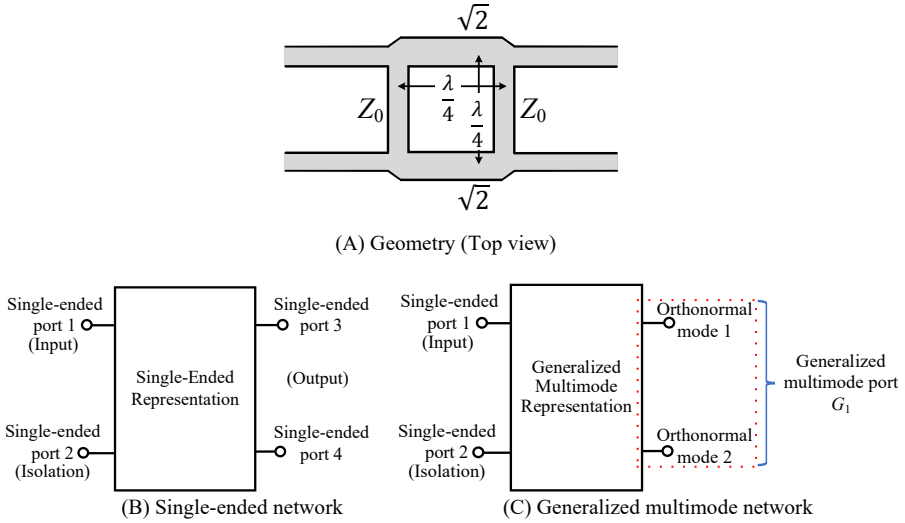

(A) Geometry (Top view)

(B) Single-ended network (C) Generalized multimode network

Figure 3 A branch-line coupler, and its single-ended and generalized multimode representations.

3 Applications of Generalized Multimode S-Parameters: Branch-Line Coupler

A simple but representative example is the branch-line coupler (BLC, or 3-dB or 90° hybrid coupler), a single-ended 4-port network[20]. Its geometry and single-ended representation are shown in Figure 3(A) and (B), respectively.

First, this section shows the design objectives of using both the single-ended and generalized multimode *S*-parameters. Then, characterize the component performance using two kinds of *S*-parameters.

3.1 Representing BLC Using Single-Ended S-Parameters

When using the single-ended *S*-parameters to design a BLC, there are three design objectives that must be considered simultaneously, which are the amplitudes of transmission coefficients from input to two output single-ended ports $|S_{31}|$ and $|S_{41}|$ being the same and maximized, and the phase difference between two output ports $\angle S_{31} - \angle S_{41}$ being 90°, as listed in Table I.

3.2 Representing BLC Using Generalized Multimode S-Parameters

Now apply the generalized multimode *S*-parameters to the same design following the steps given in Part 2.4.

Step 1: Since single-ended ports 3 and 4 are of the same type (both are output ports), they are regarded as one generalized multimode port supporting two orthonormal modes. While single-ended ports 1 and 2 are left to be single-ended. Then, the obtained generalized multimode network representation is shown in Figure 3(C).

Step2: Since the unitless complex amplitudes on the BLC's two single-ended output ports should be equal in amplitude and 90° difference in phase, define the two orthonormal modes on the generalized multimode port G_1 as follow,

$$\boldsymbol{u}_{G_1:1} = \frac{1}{\sqrt{2}}[1 \quad j]^{\mathrm{T}} \tag{11-1}$$

$$\boldsymbol{u}_{G_1:2} = \frac{1}{\sqrt{2}}[1 \quad -j]^{\mathrm{T}}. \tag{11-2}$$

Then, the orthonormal basis $\boldsymbol{B}_{G_1}^{MM}$ of the generalized multimode port G_1 is given by,

$$\boldsymbol{B}_{G_1}^{MM} = [\boldsymbol{u}_{G_1:1} \quad \boldsymbol{u}_{G_1:2}] = \frac{1}{\sqrt{2}}\begin{bmatrix} 1 & 1 \\ j & -j \end{bmatrix}. \tag{12}$$

On the other hand, the single-ended ports 1 and 2 are represented by a 2×2 unit matrix $I_{2\times 2}$. At last, the orthonormal basis $\boldsymbol{B}^{MM}$ of the overall generalized multimode network can be formed using (10), given by,

$$\boldsymbol{B}^{MM} = \begin{bmatrix} \boldsymbol{I}_{2\times 2} & \boldsymbol{0} \\ \boldsymbol{0} & \boldsymbol{B}_{G_1}^{MM} \end{bmatrix}_{4\times 4} = \frac{1}{\sqrt{2}}\begin{bmatrix} \sqrt{2} & 0 & 0 & 0 \\ 0 & \sqrt{2} & 0 & 0 \\ 0 & 0 & 1 & 1 \\ 0 & 0 & j & -j \end{bmatrix}. \tag{13}$$

Step 3: Applying (9), obtain the generalized multimode *S*-parameters $\boldsymbol{S}^{MM}$ from the single-ended ones $\boldsymbol{S}^{SE}$, given by

$$\begin{aligned} \boldsymbol{S}^{MM} &= (\boldsymbol{B}^{MM})^{\dagger}\boldsymbol{S}^{SE}\boldsymbol{B}^{MM} \\ &= \begin{bmatrix} S_{S:1,S:1} & S_{S:1,S:2} & S_{S:1,G_1:1} & S_{S:1,G_1:2} \\ S_{S:2,S:1} & S_{S:2,S:2} & S_{S:2,G_1:1} & S_{S:2,G_1:2} \\ S_{G_1:1,S:1} & S_{G_1:1,S:2} & S_{G_1:1,G_1:1} & S_{G_1:1,G_1:2} \\ S_{G_1:2,S:1} & S_{G_1:2,S:2} & S_{G_1:2,G_1:1} & S_{G_1:2,G_1:2} \end{bmatrix}. \end{aligned} \tag{14}$$

For an element of $\boldsymbol{S}^{MM}$, the subscript $G_k{:}\,i$ represents the orthonormal mode i of the generalized multimode port G_k, and $S{:}\,j$ represents the single-ended port j. Thus, $S_{G_k:i,S:j}$ means the transmission coefficient from the single-ended port j to the orthonormal mode i of the generalized multimode port G_k.

Step 4: The purpose of the design is to convert the mode on the input port, i.e., the single-ended port 1, i.e., orthonormal mode 1 defined by (11-1) on the output port (namely, the generalized multimode port G_1) as much as possible. *Therefore, when using the generalized multimode S-parameters $\boldsymbol{S}^{MM}$, there is only one design objective that is maximizing $S_{G_1:1,S:1}$*, which represents the transmission coefficient from the single-ended port 1 (input port) to the orthonormal mode 1 of the generalized multimode port G_1, as listed in Table I. From (9), $S_{G_1:1,S:1}$is obtained as follow,

$$S_{G_1:1,S:1} = \frac{1}{\sqrt{2}}\left(S_{31} - S_{41}e^{j\frac{\pi}{2}}\right). \tag{15}$$

The higher $S_{G_1:1,S:1}$ is, the better the design will be. The other three critical elements are as bellow,

$$S_{S:1,S:1} = S_{11} \tag{16-1}$$
$$S_{S:2,S:1} = S_{21} \tag{16-2}$$
$$S_{G_1:2,S:1} = \frac{1}{\sqrt{2}}\left(S_{31} + S_{41}e^{j\frac{\pi}{2}}\right). \tag{16-3}$$

$S_{S:1,S:1}$ is the reflection coefficient on the single-ended port 1(input port). $S_{S:2,S:1}$is the coupling from the single-ended port 1 to 2. $S_{G_1:2,S:1}$ is the transmission coefficient from the single-ended port 1 to orthonormal mode 2 of the generalized multimode port G_1.

In the design, though $S_{G_1:1,S:1}$and $S_{G_1:2,S:1}$ cannot be directly obtained from the measurement and simulation, one can calculate them from the single-ended *S*-parameters S_{31} and S_{41}using (15) and (16), respectively. *In this way, the three-objective problem is simplified into a single-objective one that is easy to analyze and possesses clearer physical meanings.*

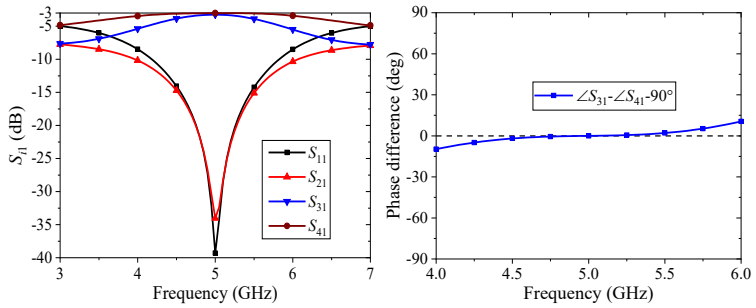

(A) Amplitude (B) Phase

Figure 4 The single-ended *S*-parameters for the optimized 5-GHz BLC.

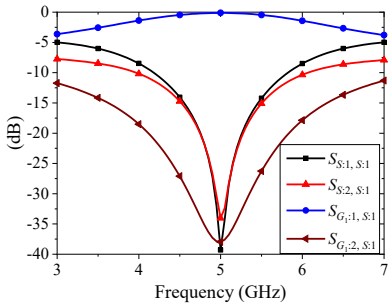

Figure 5 The generalized multimode *S*-parameters for the optimized 5-GHz BLC.

3.3 Characterizing BLC's Performance Using Generalized Multimode S-Parameters

This part takes an optimized 5-GHz lossless BLC design as an example to show how to characterize a BLC's performance using the generalized multimode *S*-parameters in the design.

All the single-ended *S*-parameters needed to characterize the BLC's performance is given in Figure 4. As can be seen, at 5 GHz, the amplitudes of S_{31} and S_{41} are the same and close to -3 dB, and the phase difference is 90°, which means the input is well converted into the desired mode on the output ports. Besides, little input power wave (<-30 dB) is reflected on the input port or transmitted to the isolation port.

All the generalized multimode *S*-parameters needed to characterize the BLC's performance is shown in Figure 5. As can be seen, at 5 GHz, $S_{G_1:1,S:1}$ is close to 0 dB, meaning the input power well converted into the desired mode (orthonormal mode 1) on the output ports. The bigger the difference between $S_{G_1:1,S:1}$ and $S_{G_1:2,S:1}$ is, the pure the desired mode on the two single-ended output ports will be. When $S_{G_1:1,S:1}$ reaches 0 dB, $S_{G_1:2,S:1}$, $S_{S:1,S:1}$ and $S_{S:2,S:1}$ will be naturally very small because of the conservation of energy.

Comparing Figures. 4 and 5, the latter using the generalized multimode *S*-parameters is obviously much simpler and clearer in showing the BLC's performance than the former using the single-ended *S*-parameters.

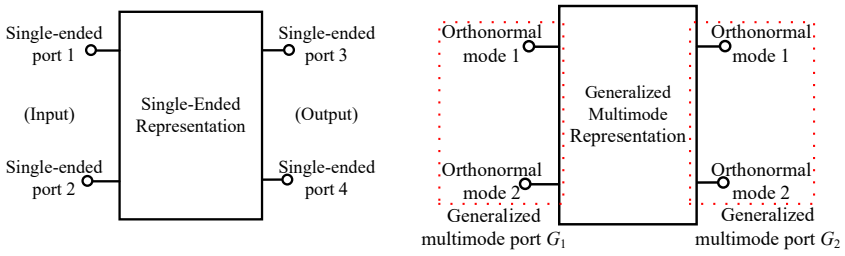

(A) Single-ended network (B) Generalized multimode network

Figure 6 The single-ended and generalized multimode representations for a standard mixed-mode 4-port network.

4 Applications of Generalized Multimode S-Parameters: Mixed-Mode S-Parameters (Verification Session)

In this section, the standard mixed-mode port case is discussed using the proposed method, which is a particular case of the generalized multimode port. The results prove the proposed method's feasibility, and it is compatible with the other previous work by using similar procedures.

Consider a single-ended 4-port network for a differential component shown in Figure 6(A), whose two single-ended ports as a differential input port and the other two as an output port. The component can be a differential filter, amplifier, or attenuator. Now apply the generalized multimode *S*-parameters following the steps given in Part 2.4.

Step 1: As already mentioned, two single-ended ports of the same type are regarded as one generalized multimode port. Each generalized multimode port supports two orthonormal modes, namely the differential and common modes. Thus, four ports of the network are regarded as two generalized multimode ports, and the generalized multimode network representation is shown in Figure 6(B).

Step 2: According to the practical application, the orthonormal modes of this case are defined as,

$$\boldsymbol{u}_{G_1:\mathrm{D}} = \frac{1}{\sqrt{2}}[1 \quad -1]^{\mathrm{T}} \tag{17-1}$$

$$\boldsymbol{u}_{G_1:\mathrm{C}} = \frac{1}{\sqrt{2}}[1 \quad 1]^{\mathrm{T}} \tag{17-2}$$

$$\boldsymbol{u}_{G_2:\mathrm{D}} = \frac{1}{\sqrt{2}}[1 \quad -1]^{\mathrm{T}} \tag{17-3}$$

$$\boldsymbol{u}_{G_2:\mathrm{C}} = \frac{1}{\sqrt{2}}[1 \quad 1]^{\mathrm{T}} \tag{17-4}$$

where $\boldsymbol{u}_{G_1:D,C}$ and $\boldsymbol{u}_{G_2:D,C}$represent the differential and common modes of the generalized multimode ports G_1 and G_2, respectively. Then the orthonormal basis $\boldsymbol{B}^{MM}$ of the overall generalized multimode network is,

$$\boldsymbol{B}^{MM} = \begin{bmatrix} \boldsymbol{B}_{G_1}^{MM} & \boldsymbol{0} \\ \boldsymbol{0} & \boldsymbol{B}_{G_2}^{MM} \end{bmatrix} = \frac{1}{\sqrt{2}} \begin{bmatrix} 1 & 1 & 0 & 0 \\ -1 & 1 & 0 & 0 \\ 0 & 0 & 1 & 1 \\ 0 & 0 & -1 & 1 \end{bmatrix}. \tag{18}$$

Step 3: From (9), the conversion from the single-ended to mixed-mode *S*-parameters is given by,

$$\begin{aligned} \boldsymbol{S}^{MM} &= (\boldsymbol{B}^{MM})^{\dagger} \boldsymbol{S}^{SE} \boldsymbol{B}^{MM} \\ &= \begin{bmatrix} S_{G_1:D,G_1:D} & S_{G_1:D,G_1:C} & S_{G_1:D,G_2:D} & S_{G_1:D,G_2:C} \\ S_{G_1:C,G_1:D} & S_{G_1:C,G_1:C} & S_{G_1:C,G_2:D} & S_{G_1:C,G_2:C} \\ S_{G_2:D,G_1:D} & S_{G_2:D,G_1:C} & S_{G_2:D,G_2:D} & S_{G_2:D,G_2:C} \\ S_{G_2:C,G_1:D} & S_{G_2:C,G_1:C} & S_{G_2:C,G_2:D} & S_{G_2:C,G_2:C} \end{bmatrix}. \end{aligned} \tag{19}$$

Step 4: Notice that if we rearrange the basis vectors to a different sequence which may lead to a different permutation of $\boldsymbol{S}^{MM}$ but would not change their values, given by,

$$\begin{aligned} \boldsymbol{B}^{MM_r} &= [\boldsymbol{u}_{G_1:\mathrm{D}} \quad \boldsymbol{u}_{G_2:\mathrm{D}} \quad \boldsymbol{u}_{G_1:\mathrm{C}} \quad \boldsymbol{u}_{G_2:\mathrm{C}}] \\ &= \frac{1}{\sqrt{2}} \begin{bmatrix} 1 & 0 & 1 & 0 \\ -1 & 0 & 1 & 0 \\ 0 & 1 & 0 & 1 \\ 0 & -1 & 0 & 1 \end{bmatrix}. \end{aligned} \tag{20}$$

Then the corresponding rearranged mixed-mode *S*-parameters would be,

$$\boldsymbol{S}^{MM_r} = (\boldsymbol{B}^{MM_r})^{\dagger} \boldsymbol{S}^{SE_r} \boldsymbol{B}^{MM_r} \tag{21}$$

which is exactly the same with simplified equations (17) and (25) deduced in Ref. 14, but does not have the restriction given by Ref. 14. Thus, the correspondence between the $\boldsymbol{B}^{MM_r}$ of this work and $\boldsymbol{M}_s$ of Ref. 14 is given below,

$$(\boldsymbol{B}^{MM_r})^{\dagger} = \mathbf{M}_s = \frac{1}{\sqrt{2}} \begin{bmatrix} 1 & -1 & 0 & 0 \\ 0 & 0 & 1 & -1 \\ 1 & 1 & 0 & 0 \\ 0 & 0 & 1 & 1 \end{bmatrix} \tag{22-1}$$

$$\boldsymbol{B}^{MM_r} = \mathbf{M}_s^{-1} = \frac{1}{\sqrt{2}} \begin{bmatrix} 1 & 0 & 1 & 0 \\ -1 & 0 & 1 & 0 \\ 0 & 1 & 0 & 1 \\ 0 & -1 & 0 & 1 \end{bmatrix}. \tag{22-2}$$

As can be seen, the proposed method is compatible with the standard mixed-mode *S*-parameters case. Besides, other mixed-mode cases investigated in previous work, such as *M* pairs of mixed-mode plus *N* single-ended ports[3] and others[1,4,21], could also be easily derived with similar procedures.

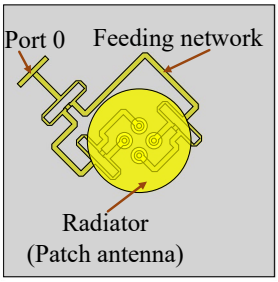

(A) SRF LHCP antenna (top view)

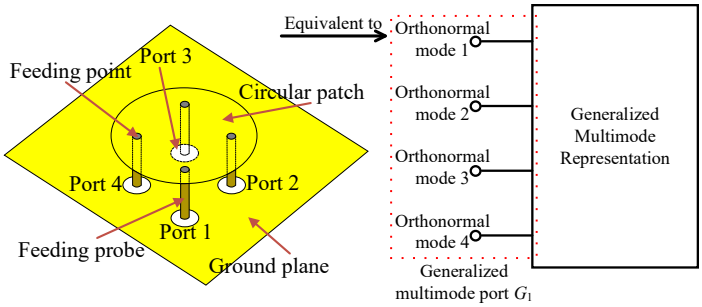

(B) 4-single-ended-port LHCP radiator (perspective view) and its generalized multimode representation

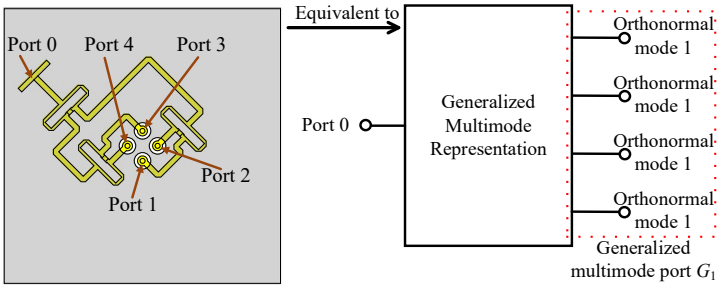

(C) 1-to-4 feeding network (top view) and its generalized multimode representation

Figure 7 A 4-element SRF LHCP patch antenna, including its 4-single-ended-port LHCP radiator and corresponding 1-to-4 feeding network.

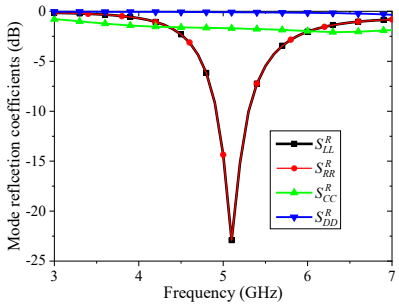

Figure 8 The mode reflection coefficients of the 4-single-ended-port SRF LHCP radiator.

5 Applications of Generalized Multimode S-Parameters: 4-Element Sequential Rotation Feeding LHCP Antenna

As already mentioned, the generalized multimode *S*-parameters have obvious advantages in analyzing and designing many different antennas and RF components. Section 3 has shown how it applies to a simple and commonly used component. Section 4

has shown how it is compatible with particular cases such as the standard mixed-mode *S*-parameters. As a more complex example, in this section, a 4-element sequential rotation feeding (SRF) left-hand circularly-polarized (LHCP) patch antenna, including its 4-single-ended-port LHCP radiator and 1-to-4 feeding network, is considered, as shown in Figure 7. The radiator and feeding network are designed using the generalized multimode *S*-parameters, respectively, which give clearer physical meanings and make the design easier when compared with that using the conventional single-ended *S*-parameters.

5.1 4-Single-Ended-Port SRF LHCP Radiator

A 4-single-ended-port symmetrically excited LHCP patch antenna radiator is shown in Figure 7(B). It has four single-ended input ports to receive four correlated signals with equal amplitude and adjacent 90° phase difference to produce a good LHCP radiation. Conventionally, for this kind of *N*-port radiators (not limited to this 4-single-ended-port SRF case), the matching performance can be assessed using accepted power calculated by the single-ended *S*-parameters[22],

$$P_{acc} = \sum_{i=1}^{N} k_i - \sum_{p=1}^{N} \left[\sum_{q=1}^{N} \sqrt{k_q}\, S_{pq} e^{j(\varphi_q - \varphi_p)} \right]^2 \tag{23}$$

where k_i and φ_i $(i = 1, 2, \dots, N)$ represent the amplitude and phase of the incident signal on the *i*th single-ended port, as listed in Table I. Although (23) provides a direct way to evaluate the overall matching performance from the perspective of the single-ended *S*-parameters, it does not possess clear physical meanings, and not all the power radiated becomes the desired LHCP- or RHCP-mode radiation.

Using the proposed procedure in Section 2, however, one will see how intuitively evaluate the mode reflection and coupling from the perspective of the generalized multimode *S*-parameters. From this, we can clearly see the impedance matchings of different combinations of the signal corresponding to different radiations (including the LHCP and RHCP radiations).

Now apply the generalized multimode *S*-parameters to the same design following the steps given in Part 2.4.

Step 1: All the four single-ended input ports are regarded as one generalized multimode port which supports four orthonormal modes, as shown in Figure 7(B).

Step 2: Different groups of bases could be adopted to express this generalized multimode port, but for this 4-single-ended-port SRF LHCP radiator, the orthonormal modes are given by,

$$\boldsymbol{u}_1^{MR} = \boldsymbol{u}_C^{MR} = \frac{1}{2}[1 \quad 1 \quad 1 \quad 1]^{\mathrm{T}} \tag{24-1}$$

$$\boldsymbol{u}_2^{MR} = \boldsymbol{u}_D^{MR} = \frac{1}{2}[1 \quad -1 \quad 1 \quad -1]^{\mathrm{T}} \tag{24-2}$$

$$\boldsymbol{u}_3^{MR} = \boldsymbol{u}_L^{MR} = \frac{1}{2}\left[1 \quad e^{j\frac{1}{2}\pi} \quad e^{j\pi} \quad e^{j\frac{3}{2}\pi}\right]^{\mathrm{T}} \tag{24-3}$$

$$\boldsymbol{u}_4^{MR} = \boldsymbol{u}_R^{MR} = \frac{1}{2}\left[1 \quad e^{-j\frac{1}{2}\pi} \quad e^{-j\pi} \quad e^{-j\frac{3}{2}\pi}\right]^{\mathrm{T}} \tag{24-4}$$

where $\boldsymbol{u}_{1\sim4}^{MR}$ corresponds to the common-, differential-, LHCP- and RHCP-mode radiation for this 4-single-ended-port SRF LHCP radiator, respectively. Due to the only one generalized multimode port, its notations in the subscript of basis are omitted to simplify. Then the orthonormal basis $\boldsymbol{B}^{MR}$ of the generalized multimode network is,

$$\boldsymbol{B}^{MR} = [\boldsymbol{u}_1^{MR} \quad \boldsymbol{u}_2^{MR} \quad \boldsymbol{u}_3^{MR} \quad \boldsymbol{u}_4^{MR}] = \frac{1}{2}\begin{bmatrix} 1 & 1 & 1 & 1 \\ 1 & -1 & j & -j \\ 1 & 1 & -1 & -1 \\ 1 & -1 & -j & j \end{bmatrix}. \tag{25}$$

Step 3: From (9), the conversion from the single-ended to generalized multimode *S*-parameters for this 4-single-ended-port SRF LHCP radiator is given by,

$$\boldsymbol{S}^{MR} = (\boldsymbol{B}^{MR})^{\dagger} \boldsymbol{S}^{SE} \boldsymbol{B}^{MR} = \begin{bmatrix} S_{CC}^R & S_{CD}^R & S_{CL}^R & S_{CR}^R \\ S_{DC}^R & S_{DD}^R & S_{DL}^R & S_{DR}^R \\ S_{LC}^R & S_{LD}^R & S_{LL}^R & S_{LR}^R \\ S_{RC}^R & S_{RD}^R & S_{RL}^R & S_{RR}^R \end{bmatrix} \tag{26}$$

where the C, D, L, R in the subscript correspond to the common-, differential-, LHCP-, and RHCP-mode radiation for this 4-single-ended-port SRF LHCP radiator, respectively. Thus, the elements of this matrix reveal the relationship between multimode modes on the generalized multimode port instead of single-ended ports, giving clear physical meanings for this 4-single-ended-port SRF

LHCP radiator's radiating waves at the same time. For example, S_{LR}^{R} represents the transmission coefficient from the RHCP to LHCP wave.

Step 4: More practically, in an ideal symmetrical situation (which is the case for all 4-single-ended-port SRF radiators), the following conditions could be used to simplify $\boldsymbol{S}^{MR}$,

$$S_{ij} = S_{ji} (i, j = 1, 2, 3, 4) \quad (27-1)$$
$$S_{12} = S_{23} = S_{34} = S_{41} \quad (27-2)$$
$$S_{13} = S_{24}. \quad (27-3)$$

Then (26) would be simplified to,

$$\boldsymbol{S}^{MR\_simp} = \begin{bmatrix} S_{11}+2S_{12}+S_{13} & 0 & 0 & 0 \\ 0 & S_{11}-2S_{12}+S_{13} & 0 & 0 \\ 0 & 0 & S_{11}-S_{13} & 0 \\ 0 & 0 & 0 & S_{11}-S_{13} \end{bmatrix}. \quad (28)$$

That is, the matrix only contains diagonal elements while the others are zero,

$$S_{CC}^{R} = S_{11} + 2S_{12} + S_{13} \quad (29-1)$$
$$S_{DD}^{R} = S_{11} - 2S_{12} + S_{13} \quad (29-2)$$
$$S_{LL}^{R} = S_{11} - S_{13} \quad (29-3)$$
$$S_{RR}^{R} = S_{11} - S_{13}. \quad (29-4)$$

The result reveals the essence that any specific mode incident wave on a symmetrically 4-single-ended-port SRF radiators would only produce the reflected wave of the same mode.

Then from the perspective of the generalized multimode *S*-parameters, the issue of optimizing the matching performance of a multiport SRF radiator could be converted to the issue of minimizing the reflection coefficient of a specific excitation mode, as listed in Table I. On the other hand, if the feeding network for the SRF radiator could provide an ideal sequential signal, then the reflection coefficients of other unwanted orthogonal modes are not needed to be considered. However, if the feeding network is not ideal, we can maximize the reflection coefficients of these modes while optimizing the radiator to improve the radiation polarization purity. In this way, even if the excitation wave of the radiator contains other unwanted modes except for the one we need, these unwanted modes would still be reflected and not excite corresponding radiations. Notice that the LHCP- and RHCP-mode reflection coefficients of the radiator are equal. This would bring up a new issue for the feeding network, which would be discussed in Part 5.3.

More specifically, consider a 4-single-ended-port SRF LHCP patch antenna radiator working at 5 GHz, as shown in Figure 7(B). The mode reflection coefficients (including the excitation mode and its orthogonal modes) are given in Figure 8. As expected, when the LHCP-mode reflection coefficient reaches a minimum in the working frequency band, both common- and differential-mode reflection coefficients are beyond -2 dB. This means most of the common- and differential-mode wave power would be reflected and not excite corresponding radiations. On the other hand, RHCP-mode excitation will be effectively radiated, as it has the same matching with LHCP one. The only way to avoid RHCP-mode radiation is minimizing RHCP-mode power in the incident wave, which relies on the feeding network design.

In this way, a new design perspective and method is developed to design and analyze a multiport SRF radiator based on the generalized multimode *S*-parameters that possess fewer design objectives and clear physical meanings than conventional methods mentioned at the beginning of this part.

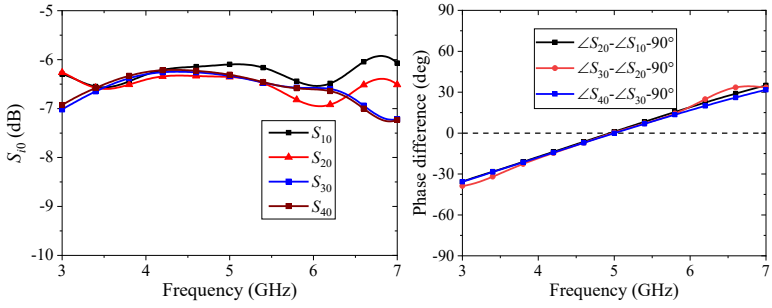

(A) Amplitude (B) Phase

Figure 9 The single-ended *S*-parameters for the 1-to-4 SRF feeding network.

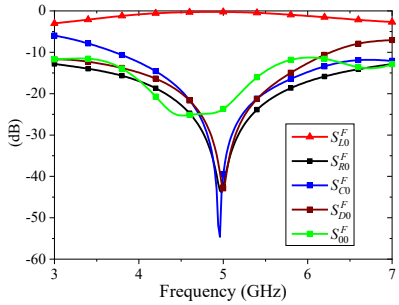

Figure 10 The transmission coefficients from input port to different generalized multi-mode modes on the generalized multi-mode port G_1.

5.2 1-to-4 Feeding Network

As already mentioned in Part 5.1, four correlated signals with equal amplitudes and adjacent 90° phase difference are needed to excite the LHCP radiator to form the SRF antenna. Conventionally, to design this kind of 1-to-*N* feeding network (not limited to this 1-to-4 case) using the single-ended *S*-parameters, there would be a large number of design objectives or variables that must be considered, including transmission coefficients from the input port to all output ports, as well as amplitude and phase unbalance on all output ports. This makes the design and analysis rather troublesome and inconvenient. Besides, the conventional method does not possess clear physical meanings. Similar to the BLC in Section 3, we could simplify the issue and give clear physical meanings from the perspective of the generalized multimode *S*-parameters.

Now apply the generalized multimode *S*-parameters to the same design following the steps given in Part 2.4. Consider the 1-to-4 LHCP-mode feeding network.

Step 1: Four single-ended output ports are regarded as one generalized multimode port supporting four orthonormal modes. The input port is left to be single-ended. Then, the obtained generalized multimode network representation is shown in Figure 7(C).

Step 2: In practical terms, the basis is given by,

$$\boldsymbol{u}_1^{MF} = \boldsymbol{u}_C^{MF} = \frac{1}{2}[1 \quad 1 \quad 1 \quad 1]^{\mathrm{T}} \tag{30-1}$$

$$\boldsymbol{u}_2^{MF} = \boldsymbol{u}_D^{MF} = \frac{1}{2}[1 \quad -1 \quad 1 \quad -1]^{\mathrm{T}} \tag{30-2}$$

$$\boldsymbol{u}_3^{MF} = \boldsymbol{u}_L^{MF} = \frac{1}{2}\left[e^{j\frac{1}{2}\pi} \quad e^{j\pi} \quad e^{j\frac{3}{2}\pi}\right]^{\mathrm{T}} \tag{30-3}$$

$$\boldsymbol{u}_4^{MF} = \boldsymbol{u}_R^{MF} = \frac{1}{2}\left[e^{-j\frac{1}{2}\pi} \quad e^{-j\pi} \quad e^{-j\frac{3}{2}\pi}\right]^{\mathrm{T}} \tag{30-4}$$

$$\boldsymbol{B}^{MF} = \frac{1}{2}\begin{bmatrix} 2 & 0 & 0 & 0 & 0 \\ 0 & 1 & 1 & 1 & 1 \\ 0 & 1 & -1 & j & -j \\ 0 & 1 & 1 & -1 & -1 \\ 0 & 1 & -1 & -j & j \end{bmatrix} \tag{30-5}$$

where $\boldsymbol{u}_{1\sim4}^{MF}$ have similar meanings with $\boldsymbol{u}_{1\sim4}^{MR}$ in Part 5.1.

Step 3: Then the conversion from the single-ended to generalized multimode *S*-parameters for this 1-to-4 feeding network is given by,

$$\boldsymbol{S}^{MF} = \begin{bmatrix} S_{00}^F & S_{0C}^F & S_{0D}^F & S_{0L}^F & S_{0R}^F \\ S_{C0}^F & S_{CC}^F & S_{CD}^F & S_{CL}^F & S_{CR}^F \\ S_{D0}^F & S_{DC}^F & S_{DD}^F & S_{DL}^F & S_{DR}^F \\ S_{L0}^F & S_{LC}^F & S_{LD}^F & S_{LL}^F & S_{LR}^F \\ S_{R0}^F & S_{RC}^F & S_{RD}^F & S_{RL}^F & S_{RR}^F \end{bmatrix} = (\boldsymbol{B}^{MF})^{\dagger}\boldsymbol{S}^{SE}\boldsymbol{B}^{MF}. \tag{31}$$

For simplification but not confusion, the generalized multimode port's notations in the subscript of basis are omitted. The C, D, L, R in the subscript of $\boldsymbol{S}^{MF}$ correspond to the output common-, differential-, LHCP-, and RHCP-mode excitation waves for this feeding network, respectively, and "0" in the subscript correspond to the single-ended port 0. For example, S_{L0}^F represent the transmission coefficient from the TEM wave on single-ended port 0 (input port) to the LHCP wave on the generalized multimode port G_1. Thus, the elements of this matrix reveal the relationships between all the multimode modes on the generalized multimode port and single-ended port 0 (input port), giving clear physical meanings for this 1-to-4 feeding network.

Step 4: Similar to Section 3, what we care about in a practical feeding network design is the reflection coefficient of the input port and transmission coefficient from the input port to different output modes, which corresponds to the elements of the first column in the matrix $\boldsymbol{S}^{MF}$, given by,

$$S_{00}^{F} = S_{00} \tag{32-1}$$

$$S_{C0}^{F} = \frac{1}{2}(S_{10} + S_{20} + S_{30} + S_{40}) \tag{32-2}$$

$$S_{D0}^{F} = \frac{1}{2}(S_{10} - S_{20} + S_{30} - S_{40}) \tag{32-3}$$

$$S_{L0}^{F} = \frac{1}{2}\left(S_{10} + S_{20}e^{j\frac{\pi}{2}} + S_{30}e^{j\pi} + S_{40}e^{-j\frac{\pi}{2}}\right) \tag{32-4}$$

$$S_{R0}^{F} = \frac{1}{2}\left(S_{10} + S_{20}e^{-j\frac{\pi}{2}} + S_{30}e^{j\pi} + S_{40}e^{j\frac{\pi}{2}}\right). \tag{32-5}$$

Having the formulas of mode reflection and transmission coefficients above, the amplitude and phase unbalance issues would be converted to maximizing a specific mode transmission coefficient, which is much more convenient, simpler, and easier to understand. In this way, we need not consider the amplitude and phase unbalance at four output ports of using the conventional single-ended *S*-parameters.

More specifically, consider a feeding network designed for the 4-single-ended-port SRF LHCP patch antenna radiator working at 5 GHz analyzed in Part 5.1, as shown in Figure 7(C). Conventionally, all the amplitudes and phases of the single-ended transmission coefficient S_{i0} $(i = 1, 2, 3, 4)$ should be considered appropriately to meet the LHCP condition, which means at least seven variables must be evaluated, as listed in Table I. Now using the generalized multimode *S*-parameters, the only variable that must be considered is the specific mode transmission coefficient from the single-ended port 0 (input port) to LHCP mode on the generalized multimode port G_1, i.e., S_{L0}^{F}, as listed in Table I. The optimized results using single-ended and generalized multimode *S*-parameters are shown in Figures. 9 and 10, respectively. As can be seen, as the single-ended *S*-parameters meeting the LHCP conditions, S_{L0}^{F} would reach the maximum within the working frequency band, while other mode transmission coefficients are getting to minimums simultaneously.

Notice that the output of the feeding network in this section is multi-way signals with equal amplitudes and unequal phases. However, the proposed procedure is also suitable for other cases, including "unequal amplitudes and equal phases" and "unequal amplitudes and unequal phases," which could obtain all possible situations.

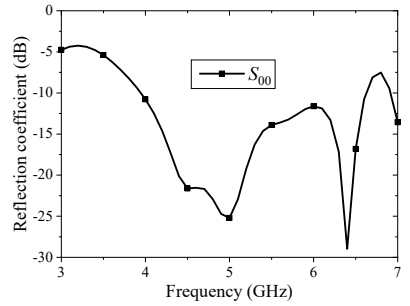

(A) Reflection coefficient of the input port

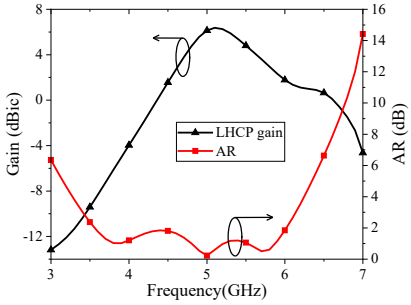

(B) Radiation performance of the whole structure

Figure 11 Reflection coefficient of the input port, LHCP-mode gain, and axial ratio (AR) of the SRF LHCP antenna.

5.3 4-Element SRF LHCP Patch Antenna with Feeding Network

As already mentioned in Part 5.1, the LHCP- and RHCP-mode reflection coefficients of the 4-single-ended-port SRF LHCP radiator are equal, and the unwanted RHCP mode is supposed not to be mixed in the excitation wave of the radiator. This problem could be naturally solved by a well-designed feeding network, in which the 0-to-RHCP mode transmission coefficient is much less than the 0-to-LHCP mode one. Thus, the RHCP-mode wave mixed in the LHCP-mode excitation wave for the radiator would not severely affect the radiation performance.

Assemble the 4-element SRF LHCP patch antenna using the radiator and feeding network designed in Part 5.1 and 5.2, as shown in Figure 7(A). In Part 5.1 and 5.2, we have optimized the multimode LHCP reflection coefficient of SRF radiator and 0-to-LHCP transmission coefficient of corresponding feeding network in working frequency band. Thus, we could expect reasonably that the cascaded structure would produce good performances for both matching and LHCP radiation, as given in Figure 11. As can be seen, the -10-dB impedance bandwidth of 4 to 6.6 GHz, 3-dB axial ratio (AR) bandwidth of 3.4 to 6.1 GHz, and 6.4 dBic peak LHCP-mode gain at center frequency all prove the feasibility of the proposed method. In particular, AR reaches 0 dB at 5 GHz, which means a pure LHCP radiation is produced at this frequency point.

It is worth mentioning that this section only gives a 4-element SRF LHCP antenna design, and SRF cases with arbitrary elements or ports could be easily deduced using a similar procedure.

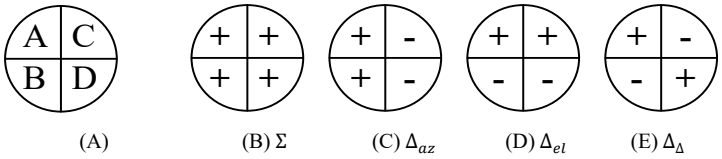

(A) (B) Σ (C) Δ_{az} (D) Δ_{el} (E) Δ_{Δ}

Figure 12 Aperture configuration of amplitude-comparison monopulse radar antenna.

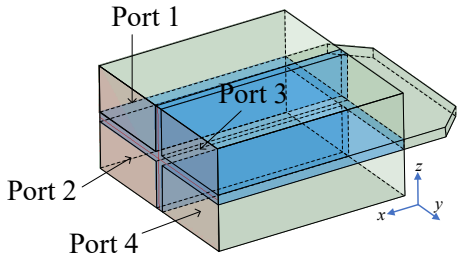

(A) Geometry (3D view)

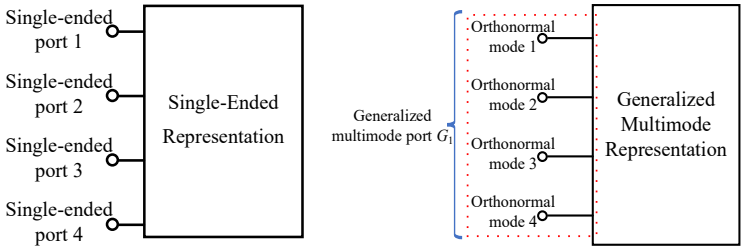

(B) Single-ended network (C) Generalized multimode network

Figure 13 A monopulse feed, and its single-ended and generalized multimode representations.

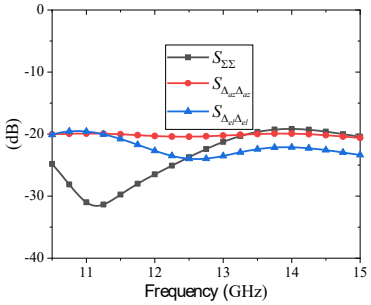

Figure 14 The mode reflection coefficients of the monopulse feed.

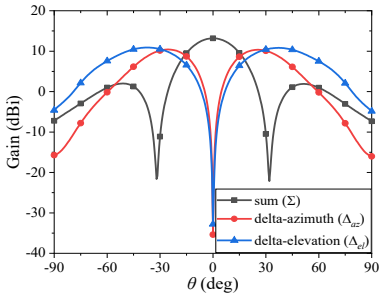

Figure 15 Sum-difference patterns of the monopulse feed.

6 Applications of Generalized Multimode S-Parameters: Monopulse Feed

Monopulse, also called a simultaneous lobe comparison, has been developed as a solution to overcome the erroneous angle indication and slow searching speed of the lobe switching and conical scan techniques used in radar tracking systems[23,24]. For an amplitude-comparison monopulse radar antenna, its feed aperture is split into four quadrants[23], as depicted in Figure 12. Each of the four quadrants is excited by one single-ended port, corresponding to four single-ended basis patterns *A*, *B*, *C*, and *D*, respectively. Thus, the monopulse feed can be regarded as a network with four single-ended ports or a network with one generalized multimode port. Four multimode far-field patterns can be obtained from the linear superposition of four single-ended basis patterns, which are sum Σ, delta-azimuth Δ_{az}, delta-elevation Δ_{el}, and delta-delta Δ_{Δ}[25], given by

$$\Sigma = \frac{1}{2}(A + B + C + D) \tag{33-1}$$

$$\Delta_{az} = \frac{1}{2}(A + B - C - D) \tag{33-2}$$

$$\Delta_{el} = \frac{1}{2}(A - B + C - D) \tag{33-3}$$

$$\Delta_{\Delta} = \frac{1}{2}(A - B - C + D). \tag{33-4}$$

The target displacement can be obtained from these four multimode far-field patterns.

Consider a monopulse feed, as shown in Figure 13(A). Conventionally, characterizing this kind of multiport radiator's overall matching performance using single-ended *S*-parameters would be very difficult and tedious. However, it will be much more convenient to analyze using generalized multimode *S*-parameters.

6.1 Representing Monopulse Feed Using Generalized Multimode S-Parameters

Now apply the generalized multimode *S*-parameters to the design following the steps given in Part 2.4.

Step 1: All four single-ended input ports are regarded as one generalized multimode port supporting four orthonormal modes. Then, the obtained generalized multimode network representation is shown in Figure 13(C).

Step 2: According to (33), the four basis vectors of the generalized multimode port could be represented as,

$$\boldsymbol{u}_{\Sigma} = \frac{1}{2}[1 \quad 1 \quad 1 \quad 1]^{\mathrm{T}} \tag{34-1}$$

$$\boldsymbol{u}_{\Delta_{az}} = \frac{1}{2}[1 \quad 1 \quad -1 \quad -1]^{\mathrm{T}} \tag{34-2}$$

$$\boldsymbol{u}_{\Delta_{el}} = \frac{1}{2}[1 \quad -1 \quad 1 \quad -1]^{\mathrm{T}} \tag{34-3}$$

$$\boldsymbol{u}_{\Delta_{\Delta}} = \frac{1}{2}[1 \quad -1 \quad -1 \quad 1]^{\mathrm{T}}. \tag{34-4}$$

And the corresponding generalized multimode basis of the network is obtained as,

$$\boldsymbol{B}^{MM} = [\boldsymbol{u}_{\Sigma} \quad \boldsymbol{u}_{\Delta_{az}} \quad \boldsymbol{u}_{\Delta_{el}} \quad \boldsymbol{u}_{\Delta_{\Delta}}] = \frac{1}{2}\begin{bmatrix} 1 & 1 & 1 & 1 \\ 1 & 1 & -1 & -1 \\ 1 & -1 & 1 & -1 \\ 1 & -1 & -1 & 1 \end{bmatrix}. \tag{35}$$

Step 3: From (9), the generalized multimode *S*-parameters for this 4-single-ended-port monopulse feed is given by,

$$\boldsymbol{S}^{MM} = (\boldsymbol{B}^{MM})^{\dagger}\boldsymbol{S}^{SE}\boldsymbol{B}^{MM} = \begin{bmatrix} S_{\Sigma\Sigma} & S_{\Sigma\Delta_{az}} & S_{\Sigma\Delta_{el}} & S_{\Sigma\Delta_{\Delta}} \\ S_{\Delta_{az}\Sigma} & S_{\Delta_{az}\Delta_{az}} & S_{\Delta_{az}\Delta_{el}} & S_{\Delta_{az}\Delta_{\Delta}} \\ S_{\Delta_{el}\Sigma} & S_{\Delta_{el}\Delta_{az}} & S_{\Delta_{el}\Delta_{el}} & S_{\Delta_{el}\Delta_{\Delta}} \\ S_{\Delta_{\Delta}\Sigma} & S_{\Delta_{\Delta}\Delta_{az}} & S_{\Delta_{\Delta}\Delta_{el}} & S_{\Delta_{\Delta}\Delta_{\Delta}} \end{bmatrix}. \tag{36}$$

Step 4: Consider the feed is symmetrical about both *xz*- and *xy*-plane, as shown in Figure 13(A), and the matrix can be simplified, where only diagonal elements $S_{ii}(i = \Sigma, \Delta_{az}, \Delta_{el}, \Delta_{\Delta})$ are non-zero. Only the the first three modes $(\Sigma, \Delta_{az}, \Delta_{el})$ are needed to be considered due to their completeness for locating the target. Due to the symmetry of the structure, the reflection coefficients of these three modes are simplified as,

$$S_{\Sigma\Sigma} = S_{11} + S_{12} + S_{13} + S_{14} \tag{37-1}$$
$$S_{\Delta_{az}\Delta_{az}} = S_{11} + S_{12} - S_{13} - S_{14} \tag{37-2}$$
$$S_{\Delta_{el}\Delta_{el}} = S_{11} - S_{12} + S_{13} - S_{14}. \tag{37-3}$$

Once $S_{ii}(i = \Sigma, \Delta_{az}, \Delta_{el})$are obtained, the design objective becomes minimizing $S_{ii}(i = \Sigma, \Delta_{az}, \Delta_{el})$ in the given bandwidth, as listed in Table I. As a comparison, characterizing the matching performance using the single-ended *S*-parameters would be rather troublesome and inconvenient, as listed in Table I. Besides, the conventional method does not possess clear physical meanings.

6.2 Characterizing Monopulse Feed's Performance Using Generalized Multimode S-Parameters

This part takes an optimized monopulse feed working at the X/Ku-band (10~15 GHz) as an example, to show how to characterize a multiport radiator's matching performance from the perspective of the generalized multimode *S*-parameters.

The generalized multimode *S*-parameters listed in (37) are given in Figure 14. As can be seen, all $S_{ii}(i = \Sigma, \Delta_{az}, \Delta_{el})$ are optimized to be less than -20 dB, representing that the monopulse feed could produce good sum (Σ), delta-elevation (Δ_{el}), and delta-delta (Δ_{Δ}) beams with little reflections. In this way, good sum-difference radiation patterns could be produced, as shown in Figure 15.

According to the analysis above and of Part 6.1, a general judging criterion is proposed for multiport radiator's matching performance based on the generalized multimode *S*-parameters. Mode reflection coefficients of the multiport radiator instead of single-ended port reflection coefficients are adopted to represent the overall reflection of the radiator. In this way, straightforward physical meanings could be obtained, and a limited small amount of design objectives are needed to be considered, which is beneficial to the multiport radiator designs.

Table I
COMPARISON OF ANTENNA AND RF COMPONENT DESIGNS USING THE SINGLE-ENDED AND GENERALIZED MULTIMODE S-PARAMETERS

Design Examples		**Design Objective(s)**	
		Single-Ended *S*-Parameters	**Generalized Multi-Mode *S*-Parameters**
Branch-Line Coupler		1. $\lvert S_{31}\rvert = \lvert S_{41}\rvert$ 2. $\lvert S_{31}\rvert = \lvert S_{41}\rvert = -3\ dB$ 3. $\angle S_{31} - \angle S_{41} = 90°$	maximizing $S_{G_1:1,S:1}$ to 0 dB
4-Element SRF Antenna	**Radiator**	$\sum_{i=1}^{N} k_i - \sum_{p=1}^{N}\left[\sum_{q=1}^{N}\sqrt{k_q}\, S_{pq} e^{j(\varphi_q - \varphi_p)}\right]^2$ or minimizing energy reflection	minimizing S_{LL}^{R}
	Feeding Network	1. $\lvert S_{10}\rvert = \lvert S_{20}\rvert = \lvert S_{30}\rvert = \lvert S_{40}\rvert$ 2. $\lvert S_{10}\rvert = \lvert S_{20}\rvert = \lvert S_{30}\rvert = \lvert S_{40}\rvert = 6\ dB$ 3. $\angle S_{20} - \angle S_{10} = \angle S_{30} - \angle S_{20} = \angle S_{40} - \angle S_{30} = 90°$	maximizing S_{L0}^{F} to 0 dB
Monopulse Feed		$\sum_{i=1}^{N} k_i - \sum_{p=1}^{N}\left[\sum_{q=1}^{N}\sqrt{k_q}\, S_{pq} e^{j(\varphi_q - \varphi_p)}\right]^2$ or minimizing energy reflection	minimizing $S_{ii}(i = \Sigma, \Delta_{az}, \Delta_{el})$

7 Discussion and Conclusion

Inspired by Meyer and Prinsloo's theory[14] and similar work in Refs. 16, 17, this paper applies the generalized multimode *S*-parameters in designing and analyzing the multiport antennas and RF components for CAD applications. Consider the special case of impedance matching which could significantly simplify the multimode representation on port, and remove the requirement on calculating port impedance. *N* single-ended ports of a network are regarded as one generalized multimode port, supporting *N* orthonormal modes represented by *N* orthonormal basis vectors, respectively. Multiport networks that are difficult to be solved or understood in single-ended manners then could be converted into much simpler multimode reflection and transmission analyses from the multimode perspective. In this way, one can only focus on the modes interested and ignore others, which leads to fewer but more intuitive physical quantities needed to be considered. This would significantly simplify the analysis, design, and optimization of some RF/microwave multiport networks, when compared with the single-ended *S*-parameters.

For better illustration, several design examples, including a conventional 3-dB 90° branch-line coupler, the standard mixed-mode case, an SRF LHCP antenna, and a monopulse feed are designed and analyzed using commercial EM CAD software Ansys HFSS with the proposed method. The method could be easily extended to any situations with arbitrary number of ports as well as other practical applications not mentioned in this paper.

Appendix: Basis, Coordinates and Transformation Matrix

Consider a general case of matrix theory[26]. Let *U* be a *n*-dimensional (*n*-D) vector space over a field (either real or complex), then $\boldsymbol{B} = [\boldsymbol{u}_1, \boldsymbol{u}_2, \cdots, \boldsymbol{u}_n]$ is called an *orthonormal basis* when

$$\langle \boldsymbol{u}_i | \boldsymbol{u}_j \rangle = \begin{cases} 1 & when\ i = j, \\ 0 & when\ i \neq j. \end{cases} \tag{A-1}$$

In this way, an arbitrary vector $\boldsymbol{x} \in U$ can be expressed as

$$\boldsymbol{x} = \alpha_1 \boldsymbol{u}_1 + \alpha_2 \boldsymbol{u}_2 + \cdots + \alpha_n \boldsymbol{u}_n = \boldsymbol{B}[\boldsymbol{x}]_{\boldsymbol{B}} \tag{A-2}$$

where the coefficients α_i uniquely determined by $\boldsymbol{B}$ are called the *coordinates of* $\boldsymbol{x}$ *with respect to* $\boldsymbol{B}$, and the $[\boldsymbol{x}]_B$ will denote the column vector, given by,

$$[\boldsymbol{x}]_{\boldsymbol{B}} = [\alpha_1 \quad \alpha_2 \quad \cdots \quad \alpha_n]^{\mathrm{T}} \tag{A-3}$$

In general, for a given vector space *U*, there exist infinite sets of orthonormal bases.

By their nature, coordinate matrix representations are basis dependent. Thus, changing the basis from one to another for a given vector space *U* may have some desirable properties. Let $\boldsymbol{B} = [\boldsymbol{u}_1, \boldsymbol{u}_2, \cdots, \boldsymbol{u}_n]$ and $\boldsymbol{B'} = [\boldsymbol{v}_1, \boldsymbol{v}_2, \cdots, \boldsymbol{v}_n]$ be two different bases for *U*, then the *transformation matrix P* with respect to the pair $(\boldsymbol{B}, \boldsymbol{B'})$ is defined to be

$$\boldsymbol{P} = [\boldsymbol{I}]_{\boldsymbol{BB'}} = [[\boldsymbol{u}_1]_{\boldsymbol{B'}} \quad [\boldsymbol{u}_2]_{\boldsymbol{B'}} \quad \cdots \quad [\boldsymbol{u}_n]_{\boldsymbol{B'}}] \tag{A-4}$$

Consider $\boldsymbol{u}_i = \alpha_{1i}\boldsymbol{v}_1 + \alpha_{2i}\boldsymbol{v}_2 + \cdots + \alpha_{ni}\boldsymbol{v}_n$, and α_{1i}~α_{ni} are complex coefficient, then the transformation matrix can be written as,

$$\boldsymbol{P} = \begin{bmatrix} \alpha_{11} & \alpha_{12} & \cdots & \alpha_{1n} \\ \alpha_{21} & \alpha_{22} & \cdots & \alpha_{2n} \\ \vdots & \vdots & \ddots & \vdots \\ \alpha_{n1} & \alpha_{n2} & \cdots & \alpha_{nn} \end{bmatrix} \tag{A-5}$$

Based on the theory above, a fundamental fact is shown that the action of a linear transformation $\boldsymbol{T}$ on a vector $\boldsymbol{u}$ is precisely matrix multiplication between the coordinates of $\boldsymbol{T}$ and the coordinates of $\boldsymbol{u}$, written as,

$$[\boldsymbol{T}(\boldsymbol{u})]_{\boldsymbol{B'}} = \boldsymbol{P}[\boldsymbol{u}]_{\boldsymbol{B}} \tag{A-6}$$

REFERENCES

1. Huynh A, Karlsson M, Gong S. Mixed-mode s-parameters and conversion techniques. Advanced Microwave Circuits and Systems. 2010;
2. Bockelman DE, Eisenstadt WR. Combined differential and common-mode scattering parameters: Theory and simulation. IEEE transactions on microwave theory and techniques. 1995;43(7):1530-1539.
3. Ferrero A, Pirola M. Generalized mixed-mode S-parameters. IEEE Transactions on Microwave Theory and Techniques. 2006;54(1):458-463.
4. Huynh A, Hakansson P, Gong S. Mixed-mode S-parameter conversion for networks with coupled differential signals. IEEE; 2007:238-241.
5. Li B, Leung KW. On the differentially fed rectangular dielectric resonator antenna. IEEE Transactions on Antennas and Propagation. 2008;56(2):353-359.
6. Liao S, Xue Q, Xu J. A Differentially Fed Magneto-electric Dipole Antenna with a Simple Structure. IEEE Antennas and Propagation Magazine. Oct. 2013;55(5):74-84. doi:10.1109/map.2013.6735476
7. Hay S, O'sullivan J. Analysis of common‐mode effects in a dual‐polarized planar connected‐array antenna. Radio Science. 2008;43(6)
8. Sun L, Li Y, Zhang Z, Wang H. Antenna Decoupling by Common and Differential Modes Cancellation. IEEE Transactions on Antennas and Propagation. 2020;
9. Shi J, Xue Q. Balanced bandpass filters using center-loaded half-wavelength resonators. IEEE transactions on microwave theory and techniques. 2010;58(4):970-977.
10. Wu C-H, Wang C-H, Chen CH. Novel balanced coupled-line bandpass filters with common-mode noise suppression. IEEE transactions on microwave theory and techniques. 2007;55(2):287-295.
11. Zhao D, Reynaert P. A 60-GHz Dual-Mode Class AB Power Amplifier in 40-nm CMOS. IEEE Journal of Solid-State Circuits. 2013;48(10):2323-2337. doi:10.1109/jssc.2013.2275662
12. Shekhar S, Walling JS, Allstot DJ. Bandwidth extension techniques for CMOS amplifiers. IEEE Journal of Solid-State Circuits. 2006;41(11):2424-2439.
13. Ahn H-T, Allstot DJ. A 0.5-8.5 GHz fully differential CMOS distributed amplifier. IEEE Journal of Solid-State Circuits. 2002;37(8):985-993.
14. Meyer P, Prinsloo DS. Generalized Multimode Scattering Parameter and Antenna Far-Field Conversions. IEEE Transactions on Antennas and Propagation. 2015;63(11):4818-4826. doi:10.1109/tap.2015.2475642
15. Prinsloo D, Meyer P, Ivashina M, Maaskant R. A quad-mode antenna for accurate polarimetric measurements over an ultra-wide field-of-view. IEEE; 2014:3260-3263.
16. Liao S, Xue Q. Compact UHF Three-Element Sequential Rotation Array Antenna for Satcom Applications. IEEE Transactions on Antennas and Propagation. 2017;65(5):2328-2338. doi:10.1109/TAP.2017.2684190
17. Liao S, Xue Q. Miniaturized VHF/UHF dual-band circularly polarized four-element sequential-rotation array antenna based on alternately overlapped bent radiation-coupled dual-L antenna elements. IEEE Transactions on Antennas and Propagation. 2018;66(9):4924-4929.
18. Zheng L, Jian-Ming J. An accurate waveguide port boundary condition for the time-domain finite-element method. IEEE Transactions on Microwave Theory and Techniques. 2005;53(9):3014-3023. doi:10.1109/tmtt.2005.854223
19. Eisenstadt WR, Thompson BM. Microwave differential circuit design using mixed-mode S-parameters. Artech house; 2006.
20. Pozar DM. Microwave engineering. John Wiley & Sons; 2012.
21. Eisenstadt WR. Microwave differential circuit design using mixed mode s-parameters. Artech House; 2006.
22. Duan W, Liao S, Zhang XY, Li YC, Xue Q. Multi-Port Patch Antennas for Flexible Power Combining and Feeding Choice. IEEE Access. 2018;6:79094-79104.
23. Sherman SM, Barton DK. Monopulse principles and techniques. Artech House; 2011.
24. Wang H, Fang D-G, Chen X. A compact single layer monopulse microstrip antenna array. IEEE Transactions on antennas and propagation. 2006;54(2):503-509.
25. Zheng Y, Tseng S-M, Yu K-B. Closed-form four-channel monopulse two-target resolution. IEEE Transactions on Aerospace and Electronic Systems. 2003;39(3):1083-1089.
26. Meyer CD. Matrix Analysis and Applied Linear Algebra. Society for Industrial and Applied Mathematics; 2000.